

# Feedback tolerant quantum dot lasers integrated with 300mm silicon photonics

Duanni Huang<sup>1\*</sup>, Shane Yerkes<sup>2</sup>, Guan-Lin Su<sup>1</sup>, Karan Mehta<sup>1</sup>, Marcus Cramer<sup>2</sup>, William O'Brien<sup>2</sup>, Razi Dehghannasiri<sup>2</sup>, Stan Dobek<sup>2</sup>, Chelsea Mackos<sup>2</sup>, Timothy Ward<sup>2</sup>, Pari Patel<sup>1</sup>, Ranjeet Kumar<sup>1</sup>, Songtao Liu<sup>1</sup>, Xinru Wu<sup>1</sup>, Xiaoxi Wang<sup>1</sup>, Junyi Gao<sup>1</sup>, Mark Isenberger<sup>2</sup>, Harel Frish<sup>2</sup>, Haisheng Rong<sup>1</sup>

1. Intel Corporation, 2200 Mission College Blvd, Santa Clara, CA 95054

2. Intel Corporation, 1600 Rio Rancho Blvd SE, Rio Rancho, NM 87124

\*duanni.huang@intel.com

**Abstract:** We demonstrate the first quantum dot lasers integrated with 300mm silicon photonics. The measured devices show a linewidth enhancement factor near zero and are resilient to optical feedback up to -16dB of back reflection.

## 1. Introduction

Quantum dot (QD) lasers have many benefits over quantum well lasers such as lower threshold current density, higher gain at elevated temperatures, reduced gain competition enabling multi-wavelength operation, and a high tolerance for optical feedback [1]. Among these many benefits, the reduced sensitivity to optical reflections has spurred the interest of many researchers lately due to the potential to realize optical isolator free operation. Removing the isolator, which is currently an essential component in optical transceivers, would reduce the packaging cost and assembly complexity.

While there has been tremendous progress in recent years to push the performance of QD lasers, most demonstrations have focused on standalone lasers rather than photonic integration to form the highly complex photonic integrated circuits (PICs) needed for transceivers. Heterogeneous integration of quantum dots with silicon photonics allows us to realize the benefits of QD lasers as well as utilize the rich library of silicon photonic waveguide devices. Furthermore, integration with silicon enables scaling to a 300mm process, allowing for advanced lithography capabilities in 300mm CMOS fabs and the potential to scale QD technology to very high volume and throughput. Previous works enabling QDs on 300mm wafers have focused on monolithic growth of QDs on silicon [2,3]. These approaches require thick buffer layers in between the QDs and silicon substrate, resulting in limited coupling of light from the laser to a silicon waveguide. Other recent QD works demonstrate coupling to silicon waveguides, but are not on 300mm wafers [4,5]. In this work, we demonstrate, to the best of our knowledge, the first hybrid silicon QD lasers integrated on a 300mm silicon photonics platform with coupling to silicon waveguide devices. We demonstrate Fabry-Perot lasers lasing up to 150C, as well as DFB lasers with >28mW of output power as well as resiliency to optical feedback up to -16dB.

## 2. Fabrication

The InAs/GaAs quantum dot epitaxial wafer is diced into small dies in preparation for bonding. Meanwhile, a 300mm SOI wafer is patterned with waveguides and gratings needed to form the laser cavities. The wafer contains grating couplers to couple light in and out, as well as doped silicon regions needed for optical attenuators, heaters, and modulators. Next, all the QD dies are bonded onto the SOI wafer as shown in Fig. 1a using direct plasma-activated bonding. A cross-section of the QD epi bonded on top of a silicon waveguide is shown in Fig. 1b. After substrate removal of the bulk GaAs, the remaining epitaxial layers are patterned using a combination of dry and wet etches to form the laser mesas and tapers between the active laser waveguide and the passive silicon waveguides. By defining the tapers after bonding, the tapers are lithographically aligned with the silicon waveguides. Finally, contact metals are deposited and patterned for the laser as well as underlying silicon devices. Images of the finished 300mm wafer are shown in Fig. 1c.

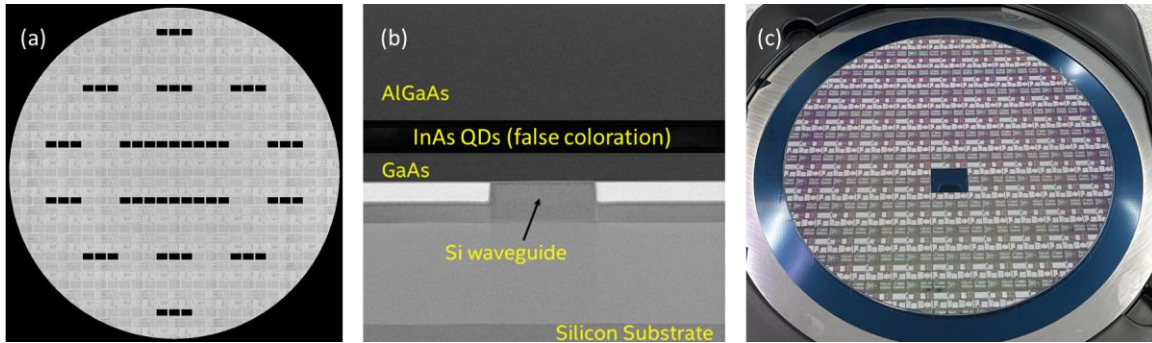


Fig. 1. (a) A 300mm SOI wafer with 54 QD die (dark rectangles) bonded on it. (b) Cross-section of the hybrid silicon QD laser with active region and silicon waveguide. (c) Picture of the wafer at end of line. One die was removed for additional testing.

### 3. Measurements

First, we measure Fabry-Perot (FP) lasers formed by a 500 $\mu\text{m}$  long gain section in between a high ( $R \sim 100\%$ ) and partial ( $R \sim 40\%$ ) reflectivity loop mirror as shown in Figs. 2a and 2b. The total cavity length including the loop mirrors is roughly 1500  $\mu\text{m}$ . The output light emitted from the grating coupler (GC) is measured using a broad-area photodetector. The QD-FP laser is tested under different stage temperatures ranging from 30 to 150C and the results are plotted in Fig. 2c. The threshold current is 20mA at 30°C and increases to 40mA at 110°C corresponding to a T0 of 115°C. The output power of the laser only drops by 0.7dB between 30 and 110°C, demonstrating the ability of the QDs to sustain its gain at elevated temperatures. Past 110°C, the laser threshold increases rapidly, and the output power drops, although it still shows clear signatures of lasing at 150°C.

Next, the QD-FP laser is studied at conditions just below threshold to observe the amplified spontaneous emission (ASE) of the device, which can be used to determine the linewidth enhancement factor (LEF), or alpha factor ( $\alpha$ ). The ASE is collected for bias currents between 10 and 20mA at which the laser begins to lase. One snapshot is shown in Fig. 2d. The ASE ripples do not blueshift with increasing current, which indicates that the real part of the modal refractive index is not changing with increased current density. After using the Hakki-Paoli method [6] to obtain the differential gain, we calculate the LEF be nearly zero between 1280 and 1320nm in Fig. 2e. In fact, it is slightly negative, which we attribute to the slight redshift in the ASE ripples due to the Joule heating. This near-zero LEF matches other predictions and experimental demonstrations of QD lasers in the literature [7]. Measurements outside of this wavelength range are limited due to the spectral bandwidth limitations of the grating coupler. The near-zero LEF implies that the laser should not enter coherence collapse until very high levels of optical feedback, due to the  $(1 + \alpha^2)/\alpha^4$  dependence of the critical feedback level on  $\alpha$  [8].

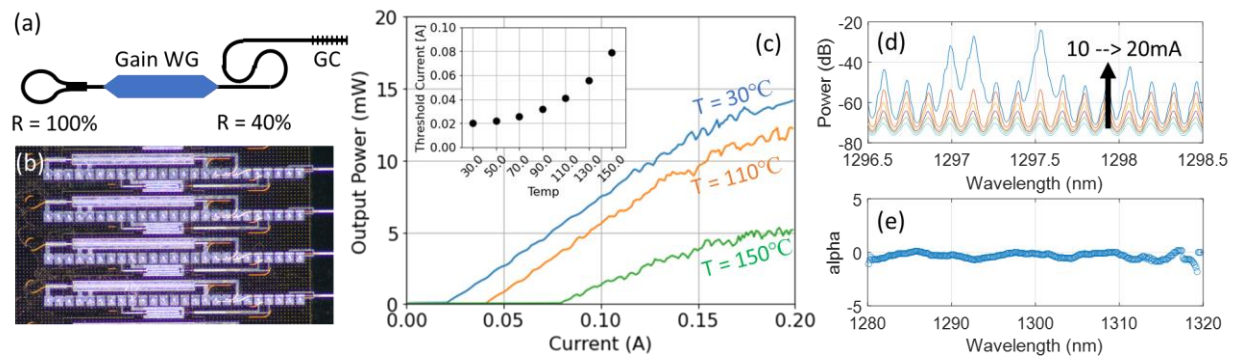


Fig. 2. (a) Schematic and (b) optical micrograph of multiple QD-FP lasers with integrated loop mirrors. (c) The L-I curves of the FP laser up to 150C. The threshold currents are plotted in the inset. (d) The amplified spontaneous emission of the laser for different subthreshold bias currents. (e) The linewidth enhancement factor, or alpha factor extracted from the measurements in (d).

This feedback insensitivity can also be measured directly by subjecting the laser to optical feedback and measuring the relative intensity noise (RIN) and side-mode suppression ratio (SMSR). For this test, we select a QD-DFB laser operating under single-mode condition. At room temperature, the 1mm long QD-DFB laser has a threshold of 26mA, and outputs 28mW of power (double-sided) at 200mA of drive current (Fig. 3a). The output

power drops by 1.5dB to 20mW and the threshold current increases to 42mA at 80°C. This power drop is higher for the QD-DFB compared to the QD-FP laser since the laser wavelength is fixed by the Bragg wavelength, which walks off from the gain peak with increasing temperature. The wavelength of the laser is 1311nm, and the SMSR is over 50 dB at 25°C. The device under test is representative of a typical QD-DFB laser on the wafer, as shown by the tight threshold current distribution across an entire wafer in Fig. 3b.

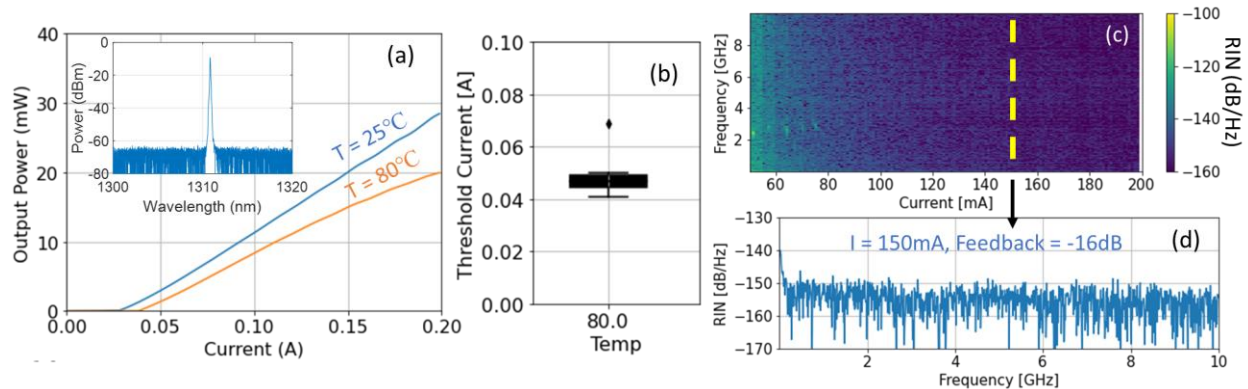


Fig. 3. (a) L-I curve for a quantum dot DFB laser at 25 and 80°C. The inset shows single-mode emission near 1310nm. (b) Threshold current statistics for the QD-DFB laser collected across the entire wafer at 80°C. (c) Colormap and (d) snapshot of the laser RIN versus bias current at -16dB optical feedback.

Next, the QD-DFB laser is tested for optical feedback tolerance by intentionally introducing a reflection through the use of an on-chip loop-mirror reflector that is placed roughly 1cm away from the laser cavity. The strength of the reflection going back to the laser is controlled using an integrated variable optical attenuator and monitored with an on-chip photodetector. This setup is capable of generating optical return loss (ORL) ranging from -30dB to -13dB. The laser bias current is also swept from slightly above threshold (50mA) to a maximum of 200mA, which effectively changes the relative phase between the reflected light and light inside the laser cavity. This ensures that a full range of both coherent and incoherent reflections are captured in the experiment.

The result of the sweep is shown in Fig. 3c at an ORL of -16dB. While some bright fringes indicating higher RIN are visible at some specific low bias currents (<80mA), the noise disappears at higher bias currents where the laser will most likely operate in a transceiver. At a typical operating current such as 150mA, the RIN is below -150dB/Hz as seen in Fig 3d, and the SMSR is completely unaffected at this feedback level. This demonstrates the feedback insensitivity characteristics of the QD-DFB, which was also predicted by the near-zero LEF.

#### 4. Conclusions

We demonstrate the first hybrid silicon quantum dot lasers integrated on a 300mm silicon photonics platform with output power larger than 28mW. The resulting devices show all the desired characteristics of quantum dots including high temperature operation up to 150°C and tolerance to optical feedback levels up to -16dB. The QD lasers show tremendous promise to be used in isolator free transceiver applications.

#### Acknowledgements

We thank Richard Jones, Ranju Venables, John Heck, Leo Varghese, Meredith Hanolsy, Yuliya Akulova, Ling Liao, Kamath Kishore, Amit Nagra, Pooya Tadayon, and James Jaussi for their support and technical guidance.

#### References

- [1] C. Shang, et al., "Perspectives on advances in quantum dot lasers and integration with Si photonic integrated circuits." *ACS Photonics* 8(9), 2555-2566, (2021).
- [2] C. Shang, et al., "Electrically pumped quantum-dot lasers grown on 300 mm patterned Si photonic wafers." *Light. Sci. Appl.* 11(1), 299 (2022).
- [3] K. Feng, et al., "Quantum Dot Lasers Directly Grown on 300 mm Si Wafers: Planar and In-Pocket." *Photonics* 10(5) (2023).
- [4] G. Kurczveil, et al., "Robust hybrid quantum dot laser for integrated silicon photonics." *Optics Express*, 24(14), 16167-16174 (2016).
- [5] Y. Wan, et al., "High speed evanescent quantum-dot lasers on Si." *Laser & Photonics Reviews* 15(8) (2021).
- [6] B. Hakki, T. Paoli., "Gain spectra in GaAs double-heterostructure injection lasers." *Journal of applied physics* 46(3), 1299-1306, (1975).
- [7] Z. Zhang, et al., "Linewidth enhancement factor in InAs/GaAs quantum dot lasers and its implication in isolator-free and narrow linewidth applications." *IEEE Journal of Selected Topics in Quantum Electronics* 25(6), 1-9, (2019).
- [8] L. Coldren, et al., "Diode Lasers and Photonic Integrated Circuits" John Wiley & Sons, (2012).